Proceedings of the 1998 IEEE
International Conference on Robotics & Automation
Leuven, Belgium • May 1998

Active leg compliance for passive walking

Richard Quint van der Linde
Delft University of Technology
Mekelweg 2
2628CD DELFT, HOLLAND

R.Q.vanderLinde@wbmt.tudelft.nl

Abstract

Previous research has shown that passive (or ballistic) walking is an energetic efficient and mechanical cheap way of walking. Therefore ballistic walking would be suitable for applications in rehabilitation technology and autonomous robots.
Successful application would require a smooth hip trajectory in order to protect respectively the patient or electronics against large velocity changes due to ground collisions.
It is shown that an actively adjustable stance leg compliance in combination with a viscous damping can result in smaller hip velocity changes.

Keywords: Biped, Ballistic, Active compliance, Limit cycle

1. Introduction

In robotics movement is often achieved by actuators servod according to a defined trajectory. Many researches have shown that it is well possible to construct a bipedal walking motion by trajectory selection in combination with servo techniques [7, 8, 12], and even realize impactless walking [2, 4].
A cyclic motion like walking can also be realized by a mechanical system oscillating in its natural orbit. This is called passive (or ballistic) walking. Using the unforced oscillation implicates that the walking motion is not solely defined by the actuators, but largely by the passive inherent system properties. Actuation is mainly present to sustain the oscillation.
It has been shown that by choosing the right geometry of the robot a stable ballistic walking cycle can be constructed [5, 6, 10]. In these researches gravity was the main power supply.
The advantages of ballistic walkers are: a minimal energy consumption, mechanical simplicity, low weight, and 'natural' walking behaviour. These advantages make ballistic walking suitable for autonomous robots and rehabilitation technology. In both areas there is an inevitable energy restriction due to autonomous functioning. Also the second area is restricted to a mechanical compact design, and an as low-as-possible weight. Ballistic walking would be a suitable technology to overcome these restrictions.
However, in its turn ballistic walking also introduces several restrictions. Since the passive walking pattern is determined by the natural frequency of the mechanical system, changing the limit cycle can only be achieved by: 1. applying an additional force or torque, 2. actively changing the intrinsic system parameters. The first solution has been studied before [1, 6, 9, 11]. In this work the latter solution has been chosen.
The most plausible intrinsic parameter to vary is joint stiffness. Active adjustment of a joint stiffness offers the ability to 1. add or withdraw energy to or from the system, 2. modify the natural frequency 3. give the system a protection against high disturbance forces. If energy storing properties are to be used also, then the compliance must be passive. By phasically changing the joint stiffness a limit cycle can be realized [15].

Successful physical application of a walking motion requires a smooth hip trajectory. This in order to protect a patient (in the case of a prosthesis or orthosis) or electronics (in the case of a robot) against impulsive forces due to ground collisions. This effect can occur at heel contact, where the weight of a biped is transferred from one leg to another. Stiff legs imply an instantaneous velocity change due to an inelastic collision. If on the other hand the legs are compliant most energy can be stored during the landing and released during the push-off. This effect is often used in running Raibert-like hoppers [14]. The advantage of a short stance phase in combination with an aerial phase allows a simple bouncing effect. The efficiency of such a collision is nearly ideal, or nearly elastic.
If the bouncing effect is used for walking robots, the spring constant must be very low due to a long stance phase. This results in an undesired large leg shortening. It can be dealt with by applying locking mechanisms [3]. However these do not result in smooth hip trajectories, and are not biologically presumable.
In this paper it is shown that smooth hip trajectories for a phasically activated passive bipedal walker can be realized by regulating leg stiffness and leg damping. The values of these parameters define three different walking modes.

2. The model

2.1 Kinematics

The model is assumed to be according Fig. 1. It is a planar compass gait model, extended with an actively variable spring (C_{SL}) and a damper (β_{SL}) in the stance leg. Both legs have a mass (m) and inertia (I_L), and a foot radius (R). The mass (M_H) of the upper body is located between the hips and is a point mass. The unsprung leg length is L_0, and the distance between the hip and the leg center of gravity is p. The model has 3 degrees of freedom; stance leg angle φ_{SL}, trailing leg angle φ_{TL}, stance leg length L_{SL}.

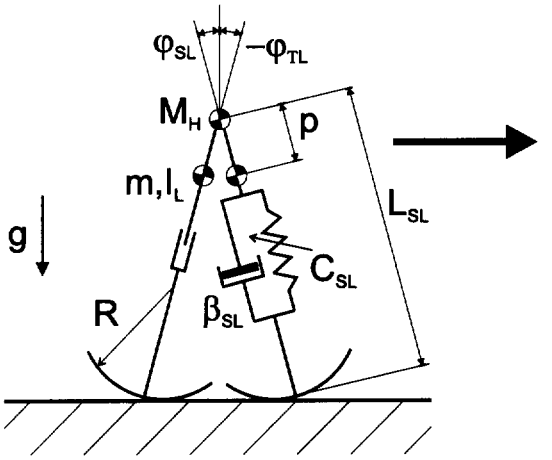

Fig. 1. *Model of the biped with actively variable leg stiffness and leg damping.*

The cycle begins when the foot of the trailing leg leaves the ground, and the system swings forward. The passive walker is activated by a stance leg stiffness change (dC), which is initiated by reaching a certain stance leg angle (φ_{PO}). This can be expressed by a dimensionless parameter :

$$\eta_{PO} = \frac{\varphi_{PO}}{\Phi_{TL}}, \qquad 0 \le \eta_{PO} \le 1 \qquad (1)$$

Where η_{PO} = dimensionless push-off parameter, φ_{PO} = push-off angle, and Φ_{TL} = trailing leg angle at push-off. The range of η_{PO} is limited, for the push-off can only occur after midstance and before foot contact. The activation phase ends when the stance phase ends.

When the foot of the trailing leg hits the floor the stance phase ends. This occurs when:

$$(L_0 - R)\cos\varphi_{TL} - (L_{SL} - R)\cos\varphi_{SL} = 0 \qquad (2)$$

Then the support leg becomes trailing leg and visa versa. After the transfer phase the next cycle begins. A complete cycle is illustrated in Fig. 2.

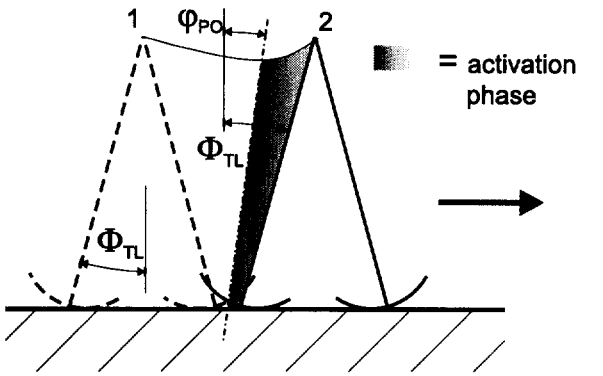

Fig. 2. *Complete walking cycle, with the gray area indicating the activation phase.*

Furthermore the following assumptions are made:

1. The lower part of the legs is massless
2. The foot of the trailing leg retracts during mid stance, so it will not scuff the floor.
3. The support transfer is instantaneous, and the foot does not slip.
4. At collision angular and linear momentum are conserved.
5. The leg stiffness change is instantaneous

2.2 Equations

Based on the model (Fig. 1) and the preceding assumptions the governing equations can be derived. Mathematically there are two distinct phases: stance phase and transfer phase.

2.2.1 Dynamics stance phase

The support phase consists of two phases: ballistic and activation. During the ballistic phase the leg stiffness C_{SL} remains a nominal stiffness C_N. In the activation phase the leg stiffness is increased from C_N to C_N+dC. Both phases are governed by the same equations of motion, with different values for C_{SL}.

The equations for stance dynamics can be given by the following general equation of motion:

$$\boldsymbol{M}(\boldsymbol{x})\ddot{\boldsymbol{x}} + \boldsymbol{N}(\boldsymbol{x},\dot{\boldsymbol{x}})\dot{\boldsymbol{x}} + \boldsymbol{G}(\boldsymbol{x}) + \boldsymbol{C}(\boldsymbol{x}) = \sum_{k=1}^{i} \boldsymbol{F}_k \frac{\partial \boldsymbol{s}_k}{\partial \boldsymbol{x}} \qquad (3)$$

Where $\boldsymbol{x} = [\varphi_{SL}\ \varphi_{TL}\ L_{SL}]^T$, $\boldsymbol{M}(\boldsymbol{x})$= 3 × 3 mass matrix, $\boldsymbol{N}(\boldsymbol{x}, \dot{\boldsymbol{x}})$= 3 × 3 coriolis matrix, $\boldsymbol{G}(\boldsymbol{x})$ = 3 × 1 gravity matrix, $\boldsymbol{C}(\boldsymbol{x})$ = 3 × 1 stiffness matrix, $\boldsymbol{F}_k$ = force $\boldsymbol{k}$ on state $\boldsymbol{x}$. $\boldsymbol{s}_k$ = direction of $\boldsymbol{F}_k$ in point of application. The matrices $\boldsymbol{M}$, $\boldsymbol{N}$, $\boldsymbol{G}$, $\boldsymbol{C}$ and the right hand expression are given as a function of system parameters in appendix A.

2.2.1 Transfer phase

The activation phase ends when the foot hits the floor. A non elastic collision occurs, during which impulse momentum is conserved. When the next cycle begins stance leg becomes trailing leg and visa versa. When the trailing leg becomes stance leg it will have unsprung length L_0. The state vector after collision can be written as:

$$x^+ = \begin{bmatrix} 0 & 1 & 0 \\ 1 & 0 & 0 \\ 0 & 0 & 1 \end{bmatrix} \cdot \begin{bmatrix} \varphi_{SL}^- \\ \varphi_{TL}^- \\ L_0 \end{bmatrix} \tag{4}$$

The impulse momentum equations can be written in the form :

$$\boldsymbol{Q}^-(\boldsymbol{x})\,\dot{\boldsymbol{x}}^- = \boldsymbol{Q}^+(\boldsymbol{x})\,\dot{\boldsymbol{x}}^+ \tag{5}$$

Where, the index "-" means before collision, the index "+" means after collision, and $\boldsymbol{Q}(\boldsymbol{x})$ = (3×3) matrix containing the impulse momentum equations. From (5) the speed and rates after collision ($\dot{\boldsymbol{x}}^+$) can be derived, which will be the initial state vector for the next cycle. $\boldsymbol{Q}^+(\boldsymbol{x})$, and $\boldsymbol{Q}^-(\boldsymbol{x})$ are given as a function of system parameters in Appendix B.

3. Cycle analysis

Limit cycles can be found by applying return map analysis. A Poincaré map is defined by the a mapping function $\boldsymbol{P}$ which maps an initial state vector $\boldsymbol{x}$ onto its self after a complete cycle [13]. A periodic (or fixed) point can then be found finding the roots of the mapping equation:

$$\boldsymbol{P}(\boldsymbol{x}) - \boldsymbol{x} = 0 \tag{6}$$

For the defined model the phase space is 6-dimensional. The end-of-step condition (2) causes 5 variables to be independent. So the mapping function is 5-dimensional. The following 5 parameters are chosen to be iterated $\dot{\varphi}_{SL}, \dot{\varphi}_{TL}, \dot{L}_{SL}, C_N$, and dC. Step width can then be given. If it is assumed that stance leg length at the end of the cycle equals L_0 then (2) is simplified by $\varphi_{SL} + \varphi_{TL} = 0$.

A Newton-Raphson method can now be used to iterate (6) until convergence. Therefore $\boldsymbol{x}$ is perturbed by $\Delta\boldsymbol{x}$ which results in:

$$\boldsymbol{x} + \Delta\boldsymbol{x} = \boldsymbol{P}(\boldsymbol{x}) + \nabla \boldsymbol{P}_{\boldsymbol{X}_0} \cdot \Delta\boldsymbol{x} + \frac{\partial \boldsymbol{P}}{\partial C_N}\Delta C_N + \frac{\partial \boldsymbol{P}}{\partial dC}\Delta dC \tag{7}$$

Where $\nabla \boldsymbol{P}_{\boldsymbol{X}_0}$ = jacobian evaluated in $\boldsymbol{X}_0$.

Rewriting this for the independent variables and iteration parameters results:

$$\begin{bmatrix} \Delta\dot{\varphi}_{SL} \\ \Delta\dot{\varphi}_{TL} \\ \Delta\dot{L}_{SL} \\ \Delta C_N \\ \Delta dC \end{bmatrix} = \left[\begin{pmatrix} \varphi_{SL} \\ L_{SL} \\ \dot{\varphi}_{SL} \\ \dot{\varphi}_{TL} \\ \dot{L}_{SL} \end{pmatrix} - \boldsymbol{P} \begin{pmatrix} \varphi_{SL} \\ L_{SL} \\ \dot{\varphi}_{SL} \\ \dot{\varphi}_{TL} \\ \dot{L}_{SL} \end{pmatrix} \right] \cdot \left(\nabla \boldsymbol{S} - \begin{bmatrix} \boldsymbol{0} & \boldsymbol{0} \\ \boldsymbol{I}\,(3\times3) & \boldsymbol{0} \end{bmatrix} \right)^{-1} \tag{8}$$

$$\text{,with } \nabla \boldsymbol{S} = \left[\frac{\partial \boldsymbol{P_X}}{\partial \dot{\varphi}_{SL}} \frac{\partial \boldsymbol{P_X}}{\partial \dot{\varphi}_{TL}} \frac{\partial \boldsymbol{P_X}}{\partial \dot{\varphi}_{SL}} \frac{\partial \boldsymbol{P_X}}{\partial C_N} \frac{\partial \boldsymbol{P_X}}{\partial dC} \right]$$

4. Simulation results

Limit cycles were found according to the mentioned analysis. The simulations were performed for the following biped configuration parameters[1] : L_0 = 0.655 [m], R = 0.2 [m], p = 0.282 [m], M_H = 1.53 [kg], m = 0.458 [kg]. I_L=.0387 [kgm^2]. These are parameters where stable passive walking can be expected [10].

The push-off parameter is chosen to be η_{PO} = 0. The dimensionless coefficient of damping is defined as

$$\beta_{SL} \equiv \kappa_{SL} / \sqrt{4 C_N \cdot M_T} \tag{9}$$

Where $M_T = 2m + M_H$ = total biped mass, κ_{SL} = stance leg damping constant [Ns/m]. Also a pre-tension U_0 is taken into account, caused by an agonist-antagonist construction [15]. In the plots U_0 is chosen to be a hypothetical 1 [m]. Later on it will be shown that it is energetically beneficial to decrease U_0, and increase dC.

Remarkable was the existence of three qualitatively different walking modes.

mode 1

A typical mode 1 cycle is characterized by the single up/down motion, illustrated in Fig. 3 for different settings of β_{SL}. Obviously the amplitude of the vertical body oscillation decreases with increase of β_{SL}. Since η_{PO} = 0 the maximum hip displacement is in midstance. The inter leg angle was chosen to be 2 × 0.23 [rad]. The gray line indicates the stiff legged compass gait hip trajectory.

[1] These parameters were largely based on the geometry of an existing prototype biped.

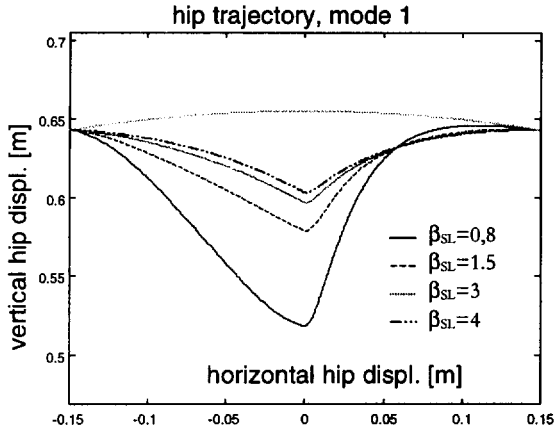

Fig. 3 *Mode 1 hip trajectory for different settings of stance leg damping:* β_{SL} *= .8, 1.5, 3, 4, and* $4<C_N \cdot L_0/M_T \cdot g<7$.

The leg stiffness range for mode 1 cycles in Fig. 3 is $4<C_N \cdot L_0/M_T \cdot g<7$. Leg activation stiffness dC increases with an increase of leg damping β_{SL}, for more energy will be lost, so more energy must be added.

mode 2

A mode 2 cycle is characterized by the double up/down motion, illustrated in Fig. 4. The resulting walking motion looks rather funny.

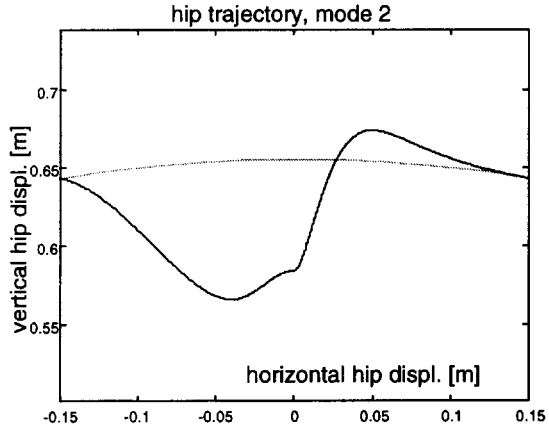

Fig. 4. *Mode 2 hip trajectory for* β_{SL} *= .2, and* $C_N \cdot L_0/M_T \cdot g=10$.

The basin of attraction appeared to be very small for this mode. Cycles were found for $C_N \cdot L_0/M_T \cdot g \approx 10$, and $\beta_{SL} \approx 0.2$. Also the cycles found were either slightly stable or slightly unstable. So this mode will most probably be very difficult to reproduce in practice.

mode 3

A mode 3 cycle is characterized by the presence of a damped vertical oscillation with small amplitude, illustrated in Fig. 5. The leg stiffness range for mode 3 cycles in Fig. 5 is $45<C_N \cdot L_0/M_T \cdot g<76$. If damping is increased to overdamped the cycle changes into a mode 1 cycle with small steps.

The nominal leg compression in the ballistic phase is approximated by $M_T \cdot g/C_N$, which is the static spring compression.

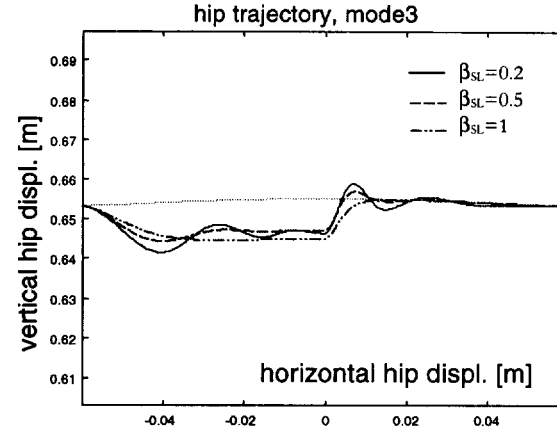

Fig. 5 *Mode 3 hip trajectory for different settings of stance leg damping:* β_{SL} *= .2, .5, 1, and* $45<C_N \cdot L_0/M_T \cdot g<76$.

A phase plane plot of the leg angle in one complete walking cycle (stance and swing) in the three different modes, and for a stiff legged biped model is given in Fig. 6. The stiff legged biped model is obtained by eliminating L_{SL} out of the state vector $\boldsymbol{x}$, and rewriting the equations (3) and (5). Energy is added by instantaneous stance leg lengthening[2].

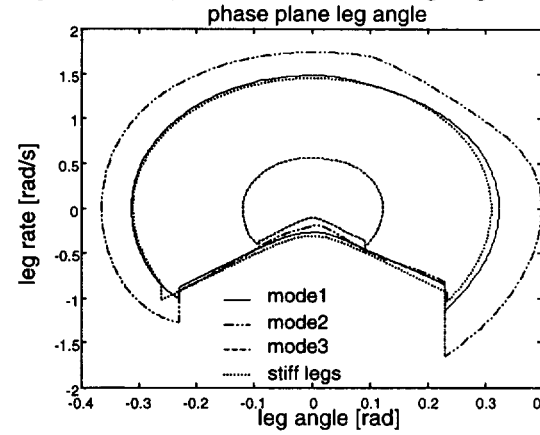

Fig. 6. *Phase plane trajectories of the leg angle for a complete walking cycle in three different modes and for a stiff legged biped model.*

The shapes of the phase plots in Fig. 6 do not differ a lot (except for the size). This can be expected, for leg angle behaviour will not be severely disrupted by a limited amount of leg lengthening.

[2] This is similar to McGeer's 'length cycling' [11]

A phase plot of the stance leg length for the three different modes is given in Fig. 7. For stiff legged walking the phase plane is not interesting , since stance leg length is assumed to change instantaneously. Fig. 7 clearly shows the difference between the three modes.

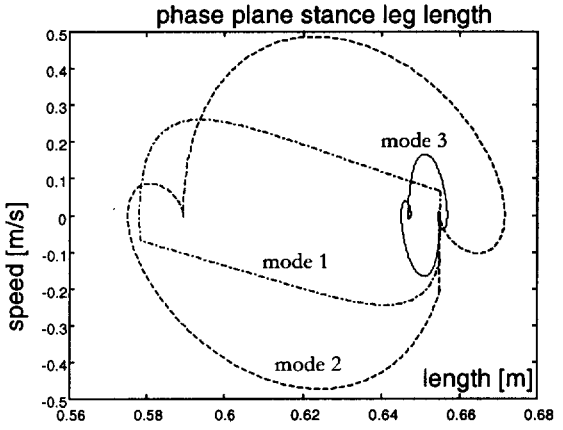

Fig. 7. *Phase plane trajectories of the leg length for a complete walking cycle in three different modes.*

Values for the vertical velocity jumps at heel contact on the hip (ΔV^Z_{HIP}) are given in table 1. These values are for an equal stance leg angle Φ_{SL} = 0.23 [rad].

Table 1. *Range of vertical velocity jumps of the hip at heel contact, for* Φ_{SL}= 0.23 [rad].

	mode 1 [m/s]	mode 2 [m/s]	mode 3 [m/s]	stiff legs [m/s]
ΔV^Z_{HIP}	0.0009 0.0084	0.013	0.005 0.007	0.22

The efficiency of transportation can be expressed by the specific resistance (SR). SR is defined as the work done divided by the product of weight and distance traveled. For the biped model the SR can be expressed as:

$$SR = \frac{energy\ input}{weight \times distance\ travelled} = \frac{\frac{1}{2}(C_N + dC)\left(L_{SL}{}^{A} - L_0 - U_0\right)^2 - \frac{1}{2}C_N\left(L_{SL}{}^{A} - L_0\right)^2}{M_T g\left\{R(\varphi_{TL-} - \varphi_{SL-}) - (L_{SL-} - R)\sin\varphi_{SL-} + (L_0 - R)\sin\varphi_{TL-}\right\}} \quad (10)$$

Where, $L_{SL}{}^{A}$ = length of the stance leg on the moment of activation, and the index '-' means just before heel contact. In order to keep SR low, U_0 must be chosen as small as possible. In order to produce an appropriate push-off force, dC then needs to be increased. By varying the ratio of U_0 and dC the specific resistance could be varied between 500 and 0.05 ! So in order to keep efficiency high it is crucial to minimize the ratio U_0 / dC.

5. Conclusions and future work

Stable ballistic walking for a biped model with active leg stiffness and damping was achieved. Three different walking modes were found, determined by the values of leg stiffness and damping.

In spite of an additional dissipating effect of damping the specific resistance can be close to that of a stiff legged walker. This is because the energy loss at foot contact is smaller than is the case for stiff legged walkers, due to energy storage of the leg spring. As a result the vertical hip amplitudes can become larger, however velocity jumps at heel contact can be decreased by a factor 244.

Since the energy input is supplied by leg extension, the passive walker is able to walk on a horizontal floor. It is also expected that the implementation of leg stiffness makes simulation results versus practice more accurate with respect to collision behaviour. Since the leg can always chosen to be less stiff than the ground, properties of the surface can vary without having significant result on the walking cycle.

A disadvantage of leg compliance is the need for larger trailing leg shortening, since the vertical hip amplitude is much larger than is the case for stiff legged walking. It might therefore be interesting to study the effect of knees in the model.

In future research a force-velocity relationship will be implemented. If pneumatic McKibben muscles are used to generate the active stiffness, this relationship will be determined. This will relate damping (derivative of force to speed) and stiffness by muscle properties. If leg stiffness is varied mode switching between the three described modes can occur.

Currently a prototype biped is being built to study the practical effect of active leg stiffness.

References

[1] Ahmadi M., Buehler M., 'Stable control of a simulated one-legged running robot with hip and leg compliance'. *IEEE trans. on Rob. and Autom* (Feb. 1997), V.13(1), pp: 96-104.

[2] Blajer W., Schiehlen W., 'Walking without impacts as a motion/force control problem'. *J. Dyn. Syst. Meas. and Contr.* (Dec. 1992), 114: 660-665.

[3] Dhandapani S., Ogot M.M. 'Modeling of a leg system to illustrate the feasibility of energy recovery in walking machines'. *ASME, Advances in Design Automation* (1994) 69(2): 429-436.

[4] Dunn E.R., Howe R.D., 'Towards smooth bipedal walking'. *Proc. IEEE Int. Conf. on Rob. and Autom.* Vol. 3, p.p. 2489-2494. May 1994, San Diego.

[5] Garcia M., Chatterjee A., Ruina, A., Coleman, 'The simplest walking model: stability, complexity, and scaling'. accepted (4-16-'97) in *ASME Journ. Biom. Eng.*

[6] Goswami A., Espiau B., Keramane A., 'Limit cycles and their stability in a passive bipedal gait'. *Int. Conf. on Rob.&Autom*(1996), pp:246-251. Minneapolis, apr. '96.

[7] Grishin A.A., Formal'sky A.M., Lensky A.V., Zhitomirsky S.V., 'Dynamic walking of a vehicle with two telescopic legs controlled by two drives'. *Int. J. Robot. Res.* (1994), 13(2): 137-147.

[8] Kajita S., Yamaura T., Kobayashi A., 'Dynamic Walking Control of a Biped Robot Along a Potential Energy Conserving Orbit'. *IEEE Trans. on Robotics and Automation* (1992), 8 (4): 431-438.

[9] McGeer T., 'Passive bipedal running'. *Proc. R. Soc. Lond. B* (1990), 204:107-134.

[10] McGeer T., 'Passive dynamic walking'. *Int. J. Robot. Res* (1990), 9(2): 62-82.

[11] McGeer T., 'Dynamics and control of bipedal locomotion'. *J. theor. Biol.* (1993), 163: 277-314.

[12] Miura H., Simoyama I., 'Dynamic walk of a biped'. *Int. J. Robot. Res.* (1984), 3(2):60-74.

[13] Seydel, R., *'Practical bifurcation and stability analysis'*. New York 1994 (2nd ed.). Springer-Verlag. ISBN: 3-540-94316-1.

[14] Raibert M., *Legged robots that balance.* Cambridge, 1986. Mass.:MIT Press. ISBN: 0-262-18117-7.

[15] Van der Linde R.Q., 'Design, analysis and control of a low power joint for walking robots, by phasic activation of McKibben muscles'. subm. to *IEEE Rob. and Autom.*

Appendix A, body dynamics matrices

The general notation of the equations of motion for the model in the stance phase is given by (3). The equations of motion were derived using LaGrange's equation:

$$\frac{d}{dt}\left(\frac{\partial \wp}{\partial \dot{\boldsymbol{x}}}\right) - \frac{\partial \wp}{\partial \boldsymbol{x}} = \sum_{k=1}^{i} \vec{F}_k \frac{\partial \vec{s}_k}{\partial \boldsymbol{x}}, \qquad \text{(A1)}$$

Where $\wp = E_{KIN} - E_{POT}$ (the LaGrange operator)
For the kinetic energy (E_{KIN}) and the potential energy (E_{POT}) we can write,

$$E_{KIN} = \tfrac{1}{2}M_H \| \boldsymbol{V}_H \|^2 + \tfrac{1}{2}m \| \boldsymbol{V}_{SL} \|^2 + \tfrac{1}{2}m \| \boldsymbol{V}_{TL} \|^2 + \tfrac{1}{2}I_L \| \dot{\varphi}_{SL} \|^2 + \tfrac{1}{2}I_L \| \dot{\varphi}_{TL} \|^2 \qquad \text{(A2)}$$

$$E_{POT} = \mu g a \cdot \cos\varphi_{SL} - mgp \cdot \cos\varphi_{TL} + M_T R g + \tfrac{1}{2}C_N(L_{SL} - L_0)^2 + \tfrac{1}{2}dC(L_{SL} - L_0 - U_0)^2 \qquad \text{(A3)}$$

$$\text{,with } \mu = M_H + \left(1 + b/a\right)m$$

Where $\boldsymbol{V_N}$ = speed vector of mass N, g = gravitation constant, U_0 = pre-tension.
Choosing a coordinate frame, expressing speeds ($\boldsymbol{V}$) in $\boldsymbol{x}$, substitute the result in A2 and A3, the matrices $\boldsymbol{M}$, $\boldsymbol{N}$, $\boldsymbol{G}$, $\boldsymbol{C}$, and $\boldsymbol{D}$ were derived by evaluating A1:

$\boldsymbol{M}(\boldsymbol{x}) = [3 \times 3]$, where

$$\begin{aligned}
M_{11} &= 2\mu R a \cdot \cos\varphi_{SL} + \lambda\left(R^2 + a^2\right) + I_L \\
M_{21} = M_{21} &= mp\left\{a \cdot \cos(\varphi_{SL} - \varphi_{TL}) + R \cdot \cos\varphi_{TL}\right\} \\
M_{31} = M_{13} &= M_T R \cdot \sin\varphi_{SL} \qquad ,M_{22} = mp^2 + I_L \\
M_{32} = M_{23} &= -mp \cdot \sin(\varphi_{SL} - \varphi_{TL}) \qquad ,M_{33} = M_T
\end{aligned}$$

$\boldsymbol{N}(\boldsymbol{x}, \dot{\boldsymbol{x}}) = [3 \times 3]$, where

$$\begin{aligned}
N_{11} &= 2L_{SL}\left\{a\mu + M_T R \cdot \cos\varphi_{SL}\right\} - \mu a R \dot{\varphi}_{SL} \cdot \sin\varphi_{SL} \\
N_{21} &= mpa\dot{\varphi}_{SL} \cdot \sin(\varphi_{SL} - \varphi_{TL}) - mpL_{SL} \cdot \cos(\varphi_{SL} - \varphi_{TL}) \\
N_{31} &= -\mu a \dot{\varphi}_{SL} \\
N_{12} &= mp\dot{\varphi}_{TL}\left\{R \cdot \sin\varphi_{SL} - a \cdot \sin(\varphi_{SL} - \varphi_{TL})\right\} \\
N_{32} &= mp\dot{\varphi}_{TL} \cdot \cos(\varphi_{SL} - \varphi_{TL}) \qquad ,N_{22} = N_{13} = N_{33} = 0 \\
N_{23} &= -mp\dot{\varphi}_{SL} \cdot \cos(\varphi_{SL} - \varphi_{TL})
\end{aligned}$$

$$\boldsymbol{G}(\boldsymbol{x}) = \begin{bmatrix} -\mu a g \cdot \sin\varphi_{SL} \\ mgp \cdot \sin\varphi_{TL} \\ M_T g \cdot \cos\varphi_{SL} \end{bmatrix}, \boldsymbol{C}(\boldsymbol{x}) = \begin{bmatrix} C_H(\varphi_{SL} - \varphi_{TL}) \\ -C_H(\varphi_{SL} - \varphi_{TL}) \\ C_N(L_{SL} - L_0) + dC(L_{SL} - L_0 - U_0) \end{bmatrix}$$

with $b = L_{SL} - p - R$, $a = L_{SL} - R$, $M_T = M_H + 2m$,

$$\lambda = M_H + \left(1 + b^2/a^2\right)m$$

$$\sum_{k=1}^{i} \vec{F}_k \frac{\partial \boldsymbol{s}_k}{\partial \boldsymbol{x}} = \begin{bmatrix} 0 & 0 & -\kappa_{SL} \cdot \dot{L} \end{bmatrix}^T$$

Appendix B, transition matrices

The transition matrices are given by:

$\boldsymbol{Q}^-(\boldsymbol{x}) = [3 \times 3]$, where

$$\begin{aligned}
Q^-_{11} &= \left\{M_H a_-^2 + 2ma_-b_-\right\}\cos\alpha_- + R\left\{\mu_- a_- - mp\right\}\cos\varphi_{SL-} \\
&\quad + R\mu_- a_- \cos\varphi_{TL-} + M_T R^2 - mpb_- + I_L \\
Q^-_{21} &= -mp\left\{R \cdot \cos\varphi_{SL-} + b_-\right\} \\
Q^-_{31} &= \mu_- a_- \cdot \sin\alpha_- + M_T R \cdot \sin\varphi_{TL-} \\
Q^-_{12} &= -mp\left\{R \cdot \cos\varphi_{TL-} + b_-\right\} \qquad ,Q^-_{22} = I_L \\
Q^-_{13} &= M_T R \cdot \sin\varphi_{SL-} - \mu_- a_- \cdot \sin\alpha \\
Q^-_{23} &= Q^-_{32} = 0 \qquad ,Q^-_{33} = M_T \cdot \cos\alpha_-
\end{aligned}$$

$\boldsymbol{Q}^+(\boldsymbol{x}) = [3 \times 3]$, where

$$\begin{aligned}
Q^+_{11} &= \lambda_+ a_+^2 + M_T R^2 + 2\mu_+ a_+ R \cdot \cos\varphi \\
&\quad - mp\left\{a_+ \cdot \cos\alpha_+ + R \cdot \cos\varphi_{T+}\right\} + I \\
Q^+_{21} &= -mp\left\{a_+ \cdot \cos\alpha_+ + R \cdot \cos\varphi_{T+}\right\} \\
Q^+_{31} &= M_T R \cdot \sin\varphi_{SL+} \\
Q^+_{12} &= -mp\left\{a_+ \cdot \cos\alpha_+ + R \cdot \cos\varphi_{TL+} - p\right\} \\
Q^+_{22} &= mp^2 + I_L \qquad ,Q^+_{32} = Q^+_{23} = mp \cdot \sin\alpha_+ \\
Q^+_{13} &= M_T R \cdot \sin\varphi_{SL+} + mp \cdot \sin\alpha_+ \qquad ,Q^+_{33} = M_T
\end{aligned}$$

Where, $\alpha_- = \varphi_{TL-} - \varphi_{SL-}$, $\alpha_+ = \varphi_{TL+} - \varphi_{SL+}$, the index '+' means post-transition, and the index '-' means pre-transition.